



## Identification of a PPAR $\delta$ agonist with partial agonistic activity on PPAR $\gamma$

Richard V. Connors<sup>a,\*</sup>, Zhulun Wang<sup>b</sup>, Martin Harrison<sup>c</sup>, Alex Zhang<sup>a</sup>, Malgorzata Wanska<sup>a</sup>, Steve Hiscock<sup>d</sup>, Brian Fox<sup>a</sup>, Michael Dore<sup>e</sup>, Marc Labelle<sup>f</sup>, Athena Sudom<sup>b</sup>, Sheree Johnstone<sup>b</sup>, Jinsong Liu<sup>b</sup>, Nigel P. C. Walker<sup>b</sup>, Anne Chai<sup>g</sup>, Karen Siegler<sup>g</sup>, Yang Li<sup>g</sup>, Peter Coward<sup>g,\*</sup>

<sup>a</sup> Department of Chemistry, Amgen, 1120 Veterans Blvd., South San Francisco, CA 94080, USA

<sup>b</sup> Department of Molecular Structure, Amgen, 1120 Veterans Blvd., South San Francisco, CA 94080, USA

<sup>c</sup> AstraZeneca Inc., Alderley Park, Cheshire SK10 4TF, UK

<sup>d</sup> Astex Therapeutics, 436 Cambridge Science Park, Milton Road, Cambridge CB4 0QA, UK

<sup>e</sup> Novartis Inc., 250 Massachusetts Ave., Cambridge, MA 02139, USA

<sup>f</sup> Lundbeck Research USA Inc., 215 College Road Paramus, NJ 07652-1431, USA

<sup>g</sup> Department of Biology, Amgen, 1120 Veterans Blvd., South San Francisco, CA 94080, USA

### ARTICLE INFO

#### Article history:

Received 26 February 2009

Revised 28 April 2009

Accepted 30 April 2009

Available online 9 May 2009

#### Keywords:

PPAR $\delta$

PPAR $\gamma$

Agonist

Modulator

### ABSTRACT

The discovery and optimization of a series of potent PPAR $\delta$  full agonists with partial agonistic activity against PPAR $\gamma$  is described.

© 2009 Elsevier Ltd. All rights reserved.

The peroxisome proliferator-activated receptors (PPARs) are members of the nuclear receptor family of ligand-regulated transcription factors.<sup>1</sup> There are three subtypes: PPAR $\alpha$  (NR1C1), PPAR $\delta$  (NR1C2, also called PPAR $\beta$ ), and PPAR $\gamma$  (NR1C3). The PPARs are essentially dietary fat sensors that maintain lipid and glucose homeostasis through control of a network of genes involved in metabolism. Their endogenous ligands include a diverse array of fatty acids, eicosanoids and oxysterols.<sup>2</sup> PPAR $\alpha$  is expressed mainly in the liver and, to a lesser degree, in muscle and heart tissue. Its principal function is control of fatty acid metabolism,<sup>3</sup> especially in response to a prolonged fast.<sup>4</sup> PPAR $\gamma$  is expressed primarily in adipose tissue, where it acts as a master regulator of adipocyte formation.<sup>5</sup> PPAR $\delta$  is expressed in many tissues, albeit at low levels in the liver. Its primary functions are control of fatty acid catabolism and energy homeostasis.<sup>6,7</sup>

Synthetic ligands have helped elucidate the biology of PPAR receptors and revealed their utility as drug targets. Fenofibrate (Tricor<sup>®</sup>), a PPAR $\alpha$  agonist that was developed as a hypolipidemic before the PPARs were discovered,<sup>8–10</sup> reduces triglycerides (TG) and free fatty acids (FFA) and raises high-density lipoprotein

(HDL). Rosiglitazone (Avandia<sup>®</sup>), a selective agonist of PPAR $\gamma$ ,<sup>11</sup> enhances insulin sensitivity, reduces plasma glucose an average of 60–80 mg/dL and exerts a moderate corrective effect on TGs, FFA and HDL in type 2 diabetes mellitus (T2DM) patients. GW501516, a selective agonist of PPAR $\delta$ , decreases low-density lipoprotein (LDL), TGs and insulin by 29%, 56% and 48%, respectively, and increases HDL by 79% in obese rhesus monkeys.<sup>12</sup> Studies in rodents suggest that activation of PPAR $\delta$  also has beneficial effects on obesity and insulin resistance.<sup>13</sup> Considerable research effort has focused on the development of selective PPAR agonists for the treatment of T2DM and metabolic syndrome.<sup>1</sup> However, the importance of controlling both lipid and glucose levels in T2DM has stimulated interest in PPAR $\alpha$ / $\gamma$ <sup>14</sup> and PPAR $\delta$ / $\gamma$ <sup>15</sup> dual agonists, as well as PPAR $\alpha$ / $\delta$ / $\gamma$  pan agonists.<sup>16</sup> As T2DM patients receiving rosiglitazone often encounter significant weight gain,<sup>11</sup> there has also been a drive to reduce this adverse effect. PPAR $\alpha$ / $\gamma$  dual agonists held promise in achieving this goal, owing to reports that fibrates reduce weight gain in rodents without impacting food intake.<sup>17</sup> Other workers have pursued PPAR $\delta$ / $\gamma$  dual agonists,<sup>18</sup> reasoning that the increased fatty acid oxidation attending PPAR $\delta$  activation<sup>19</sup> might diminish weight gain. Prompted by evidence that PPAR $\gamma$  partial agonists show a reduced weight gain profile,<sup>20</sup> we have opted to combine PPAR $\delta$  full agonism and PPAR $\gamma$  partial

\* Corresponding authors. Tel.: +1 650 244 2890 (R.V.C.).

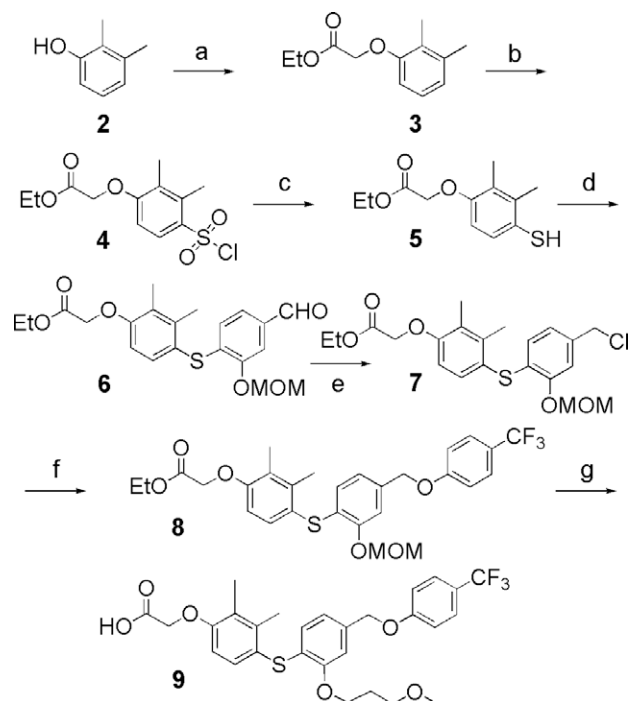
E-mail address: [rconnors@amgen.com](mailto:rconnors@amgen.com) (R.V. Connors).

agonism into a single ligand. Thus, here we describe our effort to develop a PPAR $\delta$ / $\gamma$  agonist/modulator with acceptable pharmacokinetic properties for in vivo studies.

In a recent patent,<sup>21</sup> we disclosed a class of compounds possessing potent PPAR $\delta$  agonist activity that increases HDL levels in high-fat-fed Sprague–Dawley rats. Compound **1** (Fig. 1) was selected from this series as our lead because of its favorable properties as a PPAR $\delta$ / $\gamma$  agonist/modulator. Most notably, **1** exhibits high affinity for PPAR $\delta$  ( $K_i$  = 0.007  $\mu$ M) and full agonism in the PPAR $\delta$  transactivation assay (Gal4  $EC_{50}$  = 0.018  $\mu$ M, 93% efficacy relative to GW501516<sup>12</sup>). Its affinity for PPAR $\gamma$  is weaker ( $K_i$  = 0.42  $\mu$ M) and it acts as a partial agonist in the cell based assay (Gal4  $EC_{50}$  = 0.46, 20% relative to rosiglitazone<sup>11</sup>). It is selective for PPAR $\delta$  and PPAR $\gamma$  versus PPAR $\alpha$  (PPAR $\alpha$   $K_i$  = 1.1  $\mu$ M, Gal4  $EC_{50}$  >10  $\mu$ M). Finally, **1** exhibits acceptable PK properties, with a clearance in rat of 0.06 L/h/kg and a  $V_{dss}$  of 0.7 L/kg following 0.5 mg/kg iv dosing, and an oral bioavailability of 99% after 5.0 mg/kg po dosing. Our strategy for optimizing **1** as a PPAR $\delta$ / $\gamma$  agonist/modulator was to probe the effect of substitutes for the Cl atom on the central ring, and when improved central ring analogs were identified, to prepare libraries in which the CF<sub>3</sub> aryl is diversified.

The affinity of compounds towards PPAR $\delta$  was evaluated using a scintillation proximity assay, while their affinity for PPAR $\gamma$  was assessed using a filtration assay.<sup>22</sup> The selectivity of compounds was evaluated using a PPAR $\alpha$  scintillation proximity assay as a counter-screen. Compounds exhibiting  $K_i$  values less than 0.1  $\mu$ M in the ligand binding assays were assessed for agonist activity in a transactivation assay in CV-1 cells, using a PPAR ligand binding domain/GAL4 DNA binding domain expression construct and luciferase reporter gene.<sup>23</sup>

The general synthetic route to the core structure of **1** is described in Scheme 1.<sup>24</sup> Ethyl aryloxyacetate **3** was obtained on treatment of 2,3-dimethylphenol with ethylbromoacetate in DMF/Cs<sub>2</sub>CO<sub>3</sub>. Chlorosulfonation of **3** followed by Sn reduction yielded mercaptan **5**, which was then converted to aldehyde **6** on treatment with 4-fluoro-3-methoxymethyleneoxybenzaldehyde<sup>25</sup> and Cs<sub>2</sub>CO<sub>3</sub> in DMF. Compound **7** was then obtained via NaBH<sub>4</sub> reduction of aldehyde **6**, followed by formation of the benzyl chloride with MsCl/TEA. S<sub>N</sub>2 displacement of benzyl chloride **7** with 4-hydroxybenzotrifluoride in DMF/Cs<sub>2</sub>CO<sub>3</sub> furnished compound **8**. In the final steps, the MOM protecting group in **8** was removed with 4 N HCl in dioxane, the nascent phenol was alkylated with an



**Scheme 1.** Reagents and conditions: (a) ethylbromoacetate, Cs<sub>2</sub>CO<sub>3</sub>, DMF, 50 °C, 4 h, 95%; (b) chlorosulfonic acid, 0 °C–rt, 4 h, 85%; (c) Sn, EtOH, HCl/dioxane, 0–80 °C, 4 h, 80%; (d) 4-fluoro-3-methoxymethyleneoxybenzaldehyde, Cs<sub>2</sub>CO<sub>3</sub>, DMF, 50 °C, 16 h, 60%; (e) (1) NaBH<sub>4</sub>/THF 0 °C–rt, 4 h, 95%; (2) MsCl/TEA, 0 °C–rt, 16 h, 95%; (f) 4-hydroxybenzotrifluoride, Cs<sub>2</sub>CO<sub>3</sub>, DMF, 60 °C, 16 h, 60%; (g) (1) 4N HCl/dioxane, 0 °C, 1 h, 95%; (2) Br(CH<sub>2</sub>)<sub>3</sub>OMe, Cs<sub>2</sub>CO<sub>3</sub>, DMF, 60 °C, 4 h, 80%; (3) NaOH/EtOH, 0 °C–rt, 2 h, 95%.

appropriate alkyl halide in DMF/Cs<sub>2</sub>CO<sub>3</sub> and the ethyl ester was saponified in NaOH/EtOH.

The first series of compounds examined the effect of replacing the Cl atom of **1** with ethers (Table 1). As compound **1** is already appreciably lipophilic, preference was given to low molecular weight and polar central ring substituents. In a further effort to reduce cLog P, the 2,3-dimethyl phenyl mercaptan was used in the synthesis instead of the tetrahydronaphthyl headpiece. Previous experience with **1** suggested that the 2,3-dimethyl headpiece would be tolerated but would likely modulate PPAR $\alpha$ / $\gamma$  selectivity.<sup>21</sup> As the data in Table 1 show, ligands with heteroatom-containing substituents on the central ring generally have lower activity in the  $\delta$ Gal4 functional assay. While compounds **9**, **11**, **12** and **16** all showed strong binding to PPAR $\delta$ , only weak activity was observed in the  $\delta$ Gal4 cell assay. The data in Table 1 also show a correlation between the basicity of nitrogens present in central ring substituents, PPAR $\delta$  affinity and  $\delta$ Gal4 activity. Pyridines **14** and **15**, for instance, both showed low-nM affinity for PPAR $\delta$ , while the morpholine analog **17** was 5-fold less potent and the tertiary amine **18** was inactive. All four compounds showed lower activity in the  $\delta$ Gal4 assay, while the most basic ligands **17** and **18** were inactive. Encouragingly, compound **10** stood out for its high affinity for PPAR $\delta$ , its activity in the PPAR $\delta$  cell-based assay, and its binding affinity for PPAR $\gamma$ . The cocrystal of **10** in PPAR $\delta$ <sup>26</sup> revealed a full agonist binding mode,<sup>27</sup> in which the three contiguous aryl rings wrap around helix-3 (H3), the carboxylate interacts with Y473, H323 and H449, and the CF<sub>3</sub>-aryl is positioned in close proximity to C285 (Fig. 2). The propargyl substituent projects into the central ligand binding pocket (LBP), aligned along the H7 backbone towards H5. The acetylene bond is parallel to the F368 amide carbonyl and within pi-stacking distance of the side chain phenyl.

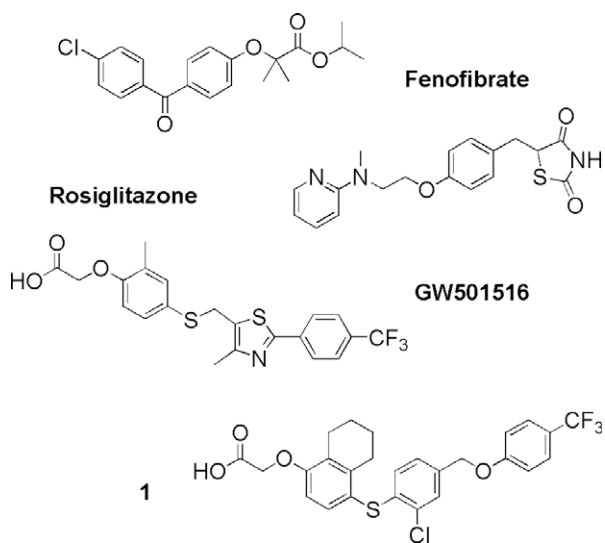
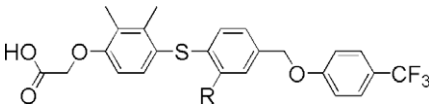


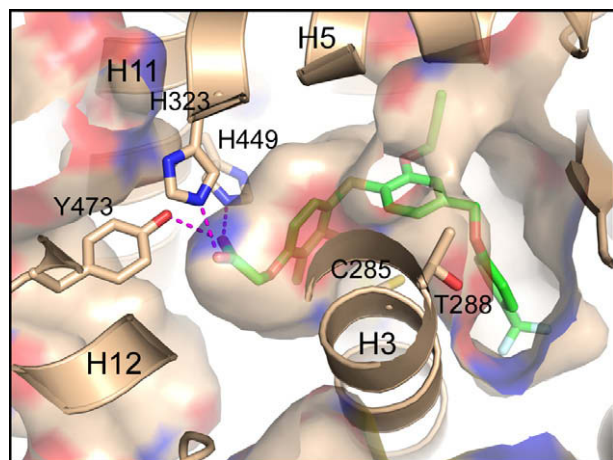
**Figure 1.** Published PPAR ligands and lead compound **1**.

**Table 1**

In vitro binding and transactivation data for the central ring side-chain ether library



Compound	<b>9</b>	<b>10</b>	<b>11</b>	<b>12</b>	<b>13</b>	<b>14</b>	<b>15</b>	<b>16</b>	<b>17</b>	<b>18</b>
αSPA K <sub>i</sub> (μM)	1.2	0.21	1.3	1.2	0.94	1.3	1.3	1.1	1.2	>10
δSPA K <sub>i</sub> (μM)	0.008	0.004	0.011	0.016	0.035	0.036	0.047	0.070	0.27	>10
γFilt K <sub>i</sub> (μM)	2.7	0.30	5.9	2.2	0.66	4.1	5.0	7.6	4.0	>10
αGal4EC <sub>50</sub> (μM) <sup>a</sup>	>10	6.1	>10	>10	>10	>10	>10	>10	>10	>10
%Max activation <sup>b</sup>	—	48%	—	—	—	—	—	—	—	—
δGal4EC <sub>50</sub> (μM) <sup>a</sup>	1.9	0.054	1.7	1.1	2.2	2.9	4.1	7.1	>10	>10
%Max activation <sup>c</sup>	88%	86%	95%	89%	95%	78%	76%	84%	—	—
γGal4EC <sub>50</sub> (μM) <sup>d</sup>	>10	3.0	>10	>10	>10	>10	>10	>10	>10	>10
%Max Activation <sup>d</sup>	—	40%	—	—	—	—	—	—	—	—

<sup>a</sup> EC<sub>50</sub> values are the molar concentrations of test compounds that afford 50% of the maximal reporter activity.<sup>b</sup> Relative to GW2433.<sup>c</sup> Relative to GW501516.<sup>d</sup> Relative to rosiglitazone.**Figure 2.** X-ray crystal structure of compound **10** in PPARδ.<sup>26</sup>

This suggests that ligands with larger central ring substituents have lower binding affinities because H7 and F368 form a relatively small pocket which is well-filled by the acetylene, but too small for larger substituents.

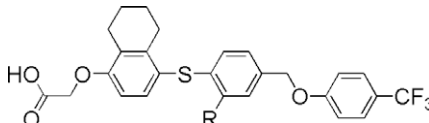
Insights derived from the compound **10** PPARδ cocrystal structure were figured into the design of the next set of compounds. As in vitro data for compound **12**<sup>21</sup> suggested that the selectivity between PPARα and PPARγ might be favorably impacted by shifting to the tetrahydronaphthyl headpiece, it was used as the scaffold in this compound set. In selecting side chain substituents, emphasis was placed on appending heteroatoms to the end of the propargyl substituent that could potentially form productive interactions with H5 in PPARδ, while exploring new binding territory in PPARγ. As the data for compound **19** in Table 2 show, shifting to the tetrahydronaphthyl headpiece does impact PPARα/γ affinity, increasing the K<sub>i</sub> for each roughly fourfold. More encouragingly, as methyl or ethyl groups are added to the propargyl terminus of **19** (**20–21**),

PPARγ affinity increases nearly 40-fold with minimal effects on PPARδ or PPARα. This trend is observed in the functional assays as well with very similar δGal4 activities for **19–21**, but with γGal4 potencies trending from 4.9 μM (43%) for compound **19** to 0.16 μM (34%) for **21**. Examination of hydroxyl-substituted analogs of **20** and **21** revealed that compound **24** possesses a nearly 10-fold increase in PPARδ affinity. The PPARδ cocrystal structures of **21** and **24** are essentially identical to that shown for **10** (Fig. 2), except for the proximity of the pentynyl hydroxyl in **24** and the F327 amide carbonyl on H5.<sup>28</sup> Despite having significant affinity for PPARδ/γ, the hydroxyl-substituted analogs are less active than **21** in the cell-based assays. Compound **21** is the best exemplar of the series, maintaining sub-μM activity in the γGal4 assay and high activity in the δGal4 assay. The cocrystal of compound **21** in PPARγ<sup>29</sup> (Fig. 3) revealed a binding geometry in which its three rings are linearly aligned along H3, with the carboxylate-AF2 interaction, known to be required for full agonism,<sup>27</sup> replaced by a close association with the R288 side chain. The pentynyl group, crucial for PPARγ affinity, occupies a hydrophobic pocket circumscribed by H3 and H7. The difference in binding mode between the two PPAR isoforms is highlighted in Figure 4.

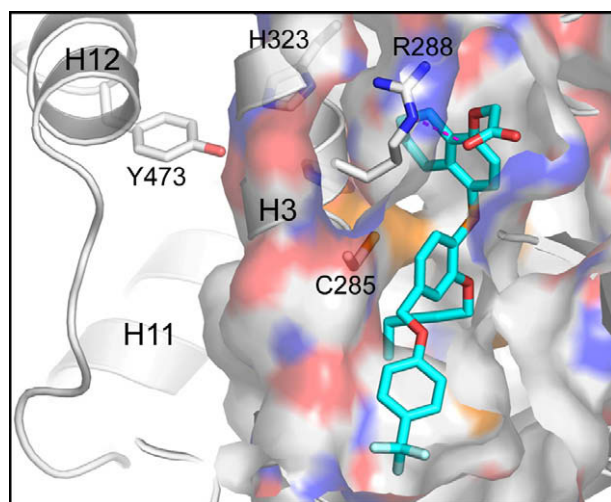
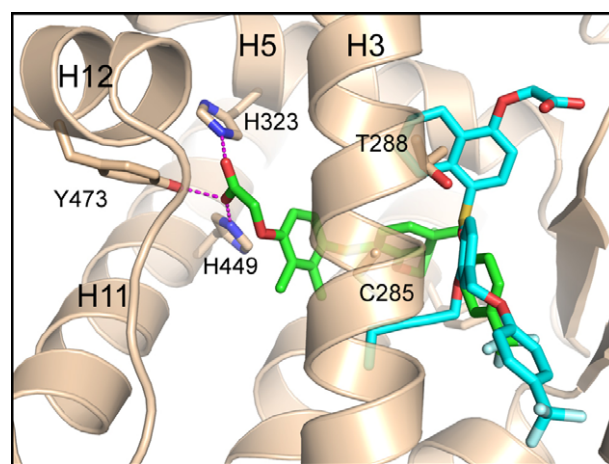
Armed with a side chain substituent conferring full agonistic activity on PPARδ and partial agonistic activity on PPARγ, attention was next directed to optimizing the CF<sub>3</sub>-aryl tailpiece. The compounds listed in Table 3 summarize the results obtained for a focused library of tailpiece variants. Shifting the tailpiece trifluoromethyl function to the *meta* and *ortho* positions progressively diminishes PPARδ affinity and functional activity. PPARγ affinity is maintained in the *meta*-substituted ligand **29** but is reduced in **30**, which is consistent with the cell-based data. Replacing the trifluoromethyl function with Cl diminishes PPARδ affinity and functional activity, as well as PPARγ cellular activity. The 2-methyl analog, **32** shows a similar profile, with concomitant loss of PPARγ affinity. Pyridyl analog **33** is less active in the PPARδ/γ cellular assays, while changing the CF<sub>3</sub>-aryl oxygen to nitrogen (compound **34**) diminishes binding to all PPAR isoforms. Saturated aliphatic substituents (**35–37**) diminish PPARδ binding, but shift γGal4 efficacy into the full agonist range. While compound **21** emerged with

**Table 2**

In vitro binding and transactivation data for the central ring alkynyl ether library



Compound	19	20	21	22	23	24	25	26	27	28
$\alpha$ SPA $K_i$ ( $\mu$ M)	0.96	1.1	0.88	1.9	1.7	1.7	2.9	2.0	1.7	1.0
$\delta$ SPA $K_i$ ( $\mu$ M)	0.007	0.006	0.005	0.022	0.002	0.0006	0.006	0.009	0.004	0.016
$\gamma$ Filt $K_i$ ( $\mu$ M)	1.2	0.077	0.033	0.084	0.21	0.043	0.079	0.020	0.044	0.025
$\alpha$ Gal4EC <sub>50</sub> ( $\mu$ M) <sup>a</sup>	3.9	>10	>10	>10	>10	>10	>10	>10	>10	>10
%Max activation <sup>b</sup>	9%	—	—	—	—	—	—	—	—	—
8Gal4EC <sub>50</sub> ( $\mu$ M) <sup>a</sup>	0.052	0.043	0.044	1.4	0.22	2.0	1.2	0.34	0.47	0.68
%Max activation <sup>c</sup>	87%	83%	94%	89%	91%	99%	99%	86%	96%	99%
$\gamma$ Gal4EC <sub>50</sub> ( $\mu$ M) <sup>a</sup>	4.9	0.70	0.16	2.2	5.9	>10	3.3	0.61	1.4	1.6
%Max activation <sup>d</sup>	43%	23%	34%	81%	79%	—	99%	21%	38%	66%

<sup>a</sup> EC<sub>50</sub> values are the molar concentrations of test compounds that afford 50% of the maximal reporter activity.<sup>b</sup> Relative to GW2433.<sup>c</sup> Relative to GW501516.<sup>d</sup> Relative to rosiglitazone.**Figure 3.** X-ray crystal structure of compound **21** in PPAR $\gamma$ .<sup>29</sup>**Figure 4.** X-ray crystal structure of compound **10** in PPAR $\delta$  with compound **21**, from an aligned PPAR $\gamma$ , superimposed.<sup>29</sup>

the best balance of PPAR $\delta$  and PPAR $\gamma$  activity of the ligands in this set, compounds such as **29**, **33** and **36** show that the tailpiece substituent can impart a range of efficacies on PPAR $\gamma$ .

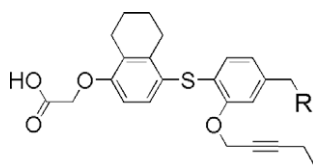
During the course of these studies, central ring and tailpiece modifications of compound **1** have yielded compound **21**, a full agonist of PPAR $\delta$  ( $K_i$  = 0.005  $\mu$ M, Gal4 EC<sub>50</sub> = 0.044 [94%]  $\mu$ M), with partial-agonist activity on PPAR $\gamma$  ( $K_i$  = 0.033  $\mu$ M, Gal4 EC<sub>50</sub> = 0.16 [34%]  $\mu$ M) and selectivity against PPAR $\alpha$  ( $K_i$  = 0.88  $\mu$ M, Gal4 EC<sub>50</sub> >10  $\mu$ M). Compound **21** displays a clearance in rat of 0.5 L/h/kg

and a Vdss of 1.4 L/kg following 0.5 mg/kg iv dosing, and an oral bioavailability of 26% after 2.0 mg/kg po dosing. Compound **21** is shown to adopt a full agonist geometry in PPAR $\delta$ ,<sup>28</sup> and a predominantly antagonist or partial agonist binding geometry in PPAR $\gamma$ .<sup>29</sup> Modification of the tailpiece aryl yields ligands with subtype selectivities ranging from PPAR $\delta$  full agonists with partial agonistic activity on PPAR $\gamma$  to PPAR $\gamma$  full agonists. These properties render compound **21** a useful tool for evaluating the in vivo effects of PPAR $\delta$  full agonism combined with partial PPAR $\gamma$  agonistic activity.



**Table 3**

In vitro binding and transactivation data for selected tailpiece aryl ether analogs



Compound	<b>21</b>	<b>29</b>	<b>30</b>	<b>31</b>	<b>32</b>	<b>33</b>	<b>34</b>	<b>35</b>	<b>36</b>	<b>37</b>
$\alpha$ SPA $K_i$ ( $\mu$ M)	0.88	1.3	0.93	2.0	0.8	7.9	5.9	5.5	2.6	4.1
$\delta$ SPA $K_i$ ( $\mu$ M)	0.005	0.035	0.12	0.036	0.028	0.011	0.66	1.2	0.15	0.12
$\gamma$ Filt $K_i$ ( $\mu$ M)	0.033	0.030	0.17	0.039	0.15	0.084	>10	0.20	0.076	0.11
$\alpha$ Gal4EC <sub>50</sub> ( $\mu$ M) <sup>a</sup>	>10	>10	>10	>10	>10	>10	>10	>10	>10	>10
%Max activation <sup>b</sup>	—	—	—	—	—	—	—	—	—	—
8Gal4EC <sub>50</sub> ( $\mu$ M) <sup>a</sup>	0.044	0.42	1.1	0.35	0.37	1.2	3.1	>10	0.90	1.5
%Max activation <sup>c</sup>	94%	83%	88%	87%	70%	99%	75%	—	95%	81%
$\gamma$ Gal4EC <sub>50</sub> ( $\mu$ M) <sup>a</sup>	0.16	0.30	4.5	0.56	0.61	0.49	—	1.5	0.50	0.39
%Max activation <sup>d</sup>	34%	26%	64%	37%	38%	65%	—	96%	92%	73%

<sup>a</sup> EC<sub>50</sub> values are the molar concentrations of test compounds that afford 50% of the maximal reporter activity.<sup>b</sup> Relative to GW2433.<sup>c</sup> Relative to GW501516.<sup>d</sup> Relative to rosiglitazone.

## References and notes

- Willson, T. M.; Brown, P. J.; Sternbach, D. D.; Henke, B. R. *J. Med. Chem.* **2000**, *43*, 527.
- Evans, R. M.; Barish, G. D.; Wang, Y.-X. *Nat. Med.* **2004**, *10*, 355.
- Reddy, J. K.; Hashimoto, T. *Annu. Rev. Nutr.* **2001**, *21*, 193.
- Kersten, S.; Seydoux, J.; Peters, J. M.; Gonzalez, F. J.; Desvergne, B.; Wahli, W. *J. Clin. Invest.* **1999**, *103*, 1489.
- Rosen, E. D.; Walkey, C. J.; Puigserver, P.; Spiegelman, B. M. *Gene Dev.* **2000**, *14*, 1293.
- Peters, J. M.; Lee, S. S. T.; Li, W.; Ward, J. M.; Gavrilova, O.; Everett, C.; Reitman, E. L.; Hudson, L. D.; Gonzalez, F. J. *Mol. Cell Biol.* **2000**, *20*, 5119.
- Barak, Y.; Liao, D.; He, W.; Ong, E. S.; Nelson, M. C.; Olefsky, J. M.; Boland, R.; Evans, R. M. *Proc. Natl. Acad. Sci.* **2002**, *99*, 303.
- Schoonjans, K.; Staels, B.; Auwerx, J. *J. Lipid. Res.* **1996**, *37*, 907.
- Balfour, J. A.; McTavish, D.; Heel, R. C. *Drugs* **1990**, *40*, 260.
- Gotto, A. M., Jr. *Am. J. Cardiol.* **1998**, *82*, 22Q.
- (a) Lehmann, J. M.; Moore, L. B.; Smith-Oliver, T. A.; Wilkison, W. O.; Willson, T. M.; Kliewer, S. A. *J. Biol. Chem.* **1995**, *270*, 12953; (b) Mudaliar, S.; Henry, R. R. *Annu. Rev. Med.* **2001**, *52*, 239.
- Oliver, W. R.; Shenk, J. L.; Snaith, M. R.; Russel, C. S.; Plunket, K. D.; Bodkin, N. L.; Lewis, M. C.; Winegar, D. A.; Sznaidman, M. L.; Lambert, M. H.; Xu, H. E.; Sternbach, D. D.; Kliewer, S. A.; Hansen, B. C.; Willson, T. M. *Proc. Natl. Acad. Sci. U.S.A.* **2001**, *98*, 5306.
- Takahashi, S.; Tanaka, T.; Kodama, T.; Sakai, J. *Pharmacol. Res.* **2006**, *53*, 501.
- Henke, B. R. *J. Med. Chem.* **2004**, *47*, 4118.
- Liu, K. G.; Lambert, M. H.; Leesnitzer, L. M.; Oliver, W.; Ott, R. J.; Plunkett, K. D.; Stuart, L. W.; Brown, P. J.; Willson, T. M.; Sternbach, D. D. *Bioorg. Med. Chem. Lett.* **2001**, *11*, 2959.
- Evans, J. L.; Lin, J. J.; Goldfine, I. D. *Curr. Diab. Rev.* **2005**, *1*, 299.
- (a) Vazquez, M.; Merlos, M.; Adzet, T.; Laguna, J. C. *Br. J. Pharmacol.* **1996**, *117*, 1155; (b) Chaput, E.; Saladin, R.; Silvestre, M.; Edgar, A. D. *Biochem. Biophys. Res. Commun.* **2000**, *271*, 445.
- Wang, Y. X.; Lee, C. H.; Broderick, C. L.; Canada, E.; Gonzalez, I.; Lamar, J.; Montrose-Rafizadeh, C.; Oldham, B. A.; Osborn, J. J.; Xie, C.; Shi, Q.; Winneroski, L. L.; York, J.; Yumibe, N.; Zink, R.; Mantlo, N. J. *Med. Chem.* **2006**, *49*, 5649.
- (a) Wang, Y. X.; Lee, C. H.; Tiep, S.; Yu, R. T.; Ham, J.; Kang, H.; Evans, R. M. *Cell* **2003**, *113*, 159; (b) Tanaka, T.; Yamamoto, J.; Iwasaki, S.; Asaba, H.; Hamura, H.; Ikeda, Y.; Watanabe, M.; Magoori, K.; Ioka, R. X.; Tachibana, K.; Watanabe, Y.; Uchiyama, Y.; Sumi, K.; Iguchi, H.; Ito, S.; Doi, T.; Hamakubo, T.; Naito, M.; Auwerx, J.; Yanagisawa, M.; Kodama, T.; Sakai, J. *Proc. Natl. Acad. Sci. U.S.A.* **2003**, *100*, 15924.
- (a) Terrie-Anne Cock, T. A.; Houten, S. M.; Auwerx, J. *EMBO Rep.* **2004**, *1*, 142; (b) Liu, K.; Black, R. M.; Acton, J. J., III; Mosley, R.; Debenham, S.; Abola, R.; Yang, M.; Tschirret-Guth, R.; Colwell, L.; Liu, C.; Wu, M.; Wang, C. F.; MacNaul, K. L.; McCann, M. E.; Moller, D. E.; Berger, J. P.; Meinke, P. T.; Jones, A. B.; Wood, H. B. *Bioorg. Med. Chem. Lett.* **2005**, *15*, 2437; (c) Acton, J. J., III; Black, R. M.; Jones, A. B.; Moller, D. E.; Colwell, L.; Doeber, T. W.; MacNaul, K. L.; Berger, J.; Wood, H. B. *Bioorg. Med. Chem. Lett.* **2005**, *15*, 357.
- Abe, H.; Houze, J.; Kawasaki, H.; Kayser, F.; Sharma, R.; Sperry, S. WO2003024395.
- hPPAR $\delta$  ligand binding was directly measured using a scintillation proximity assay. 0.1 ng/ $\mu$ l protein, 10 nM radioligand ( $[^3\text{H}]$ -GW2433, 50 Ci/mmol, 1 mCi/ml) and 0.1  $\mu$ g/ $\mu$ l polylysine SPA beads were incubated for 1 h at room temperature in binding buffer (10 mM K<sub>2</sub>HPO<sub>4</sub>, 10 mM KH<sub>2</sub>PO<sub>4</sub>, 2 mM EDTA, 50 mM NaCl, 10% (v/v) glycerol, 2 mM CHAPS, and 1 mM DTT, pH 7.1). Plates were read on a Packard TopCount. Conditions for hPPAR $\alpha$  were the same as hPPAR $\delta$  except that 2 ng/ $\mu$ l protein and 2  $\mu$ g/ $\mu$ l beads were used. For hPPAR $\gamma$ , ligand binding was directly measured using a filtration assay. 2.4 ng/ $\mu$ l protein, 20 nM 3H-rosiglitazone (20 Ci/mmol, 1 mCi/ml), and 10% glutathione bead slurry were incubated for 1 h at room temperature in binding buffer (10 mM Tris-HCl, 50 mM KCl, 1 mM DTT, 0.01% NP-40, and 0.02% BSA, pH 8.0) in a Uni-Filter 350 96-well assay plate (Polyfiltronics). The reactions were filtered under vacuum and washed twice with binding buffer. Scintillant was added and plates were read on a Packard TopCount.
- CV1 cells were plated at 15,000 cells/well in 96-well plates in DMEM/F12 + 10% charcoal/dextran-treated FBS. Cells were transfected with plasmid DNA encoding the DNA-binding domain of the yeast transcription factor GAL4 fused to the ligand binding domain of hPPAR $\alpha$ , hPPAR $\delta$ , or hPPAR $\gamma$ , and a luciferase reporter gene driven by four copies of the Gal4 promoter. Effectene was used as the transfection reagent. Four hours post-transfection, test compounds were added, and luciferase activity was measured 20 h later.
- All compounds were characterized by  $^1\text{H}$  NMR and LC/MS and their purity determined to be greater than 95% by reverse phase HPLC.
- 4-Fluoro-3-methoxymethyleneoxybenzaldehyde was prepared from 4-fluoro-3-methoxybenzaldehyde via BBr<sub>3</sub> demethylation followed by protection of the resulting phenol with MOM-Cl/TEA.
- PPAR $\delta$  X-ray structure of compound **10** (3GZ9).
- Nagy, L.; Schwabe, W. R. *Trends Biochem. Sci.* **2004**, *29*, 317.
- Unpublished results.
- PPAR $\gamma$  X-ray structure of compound **21** (3H0A).